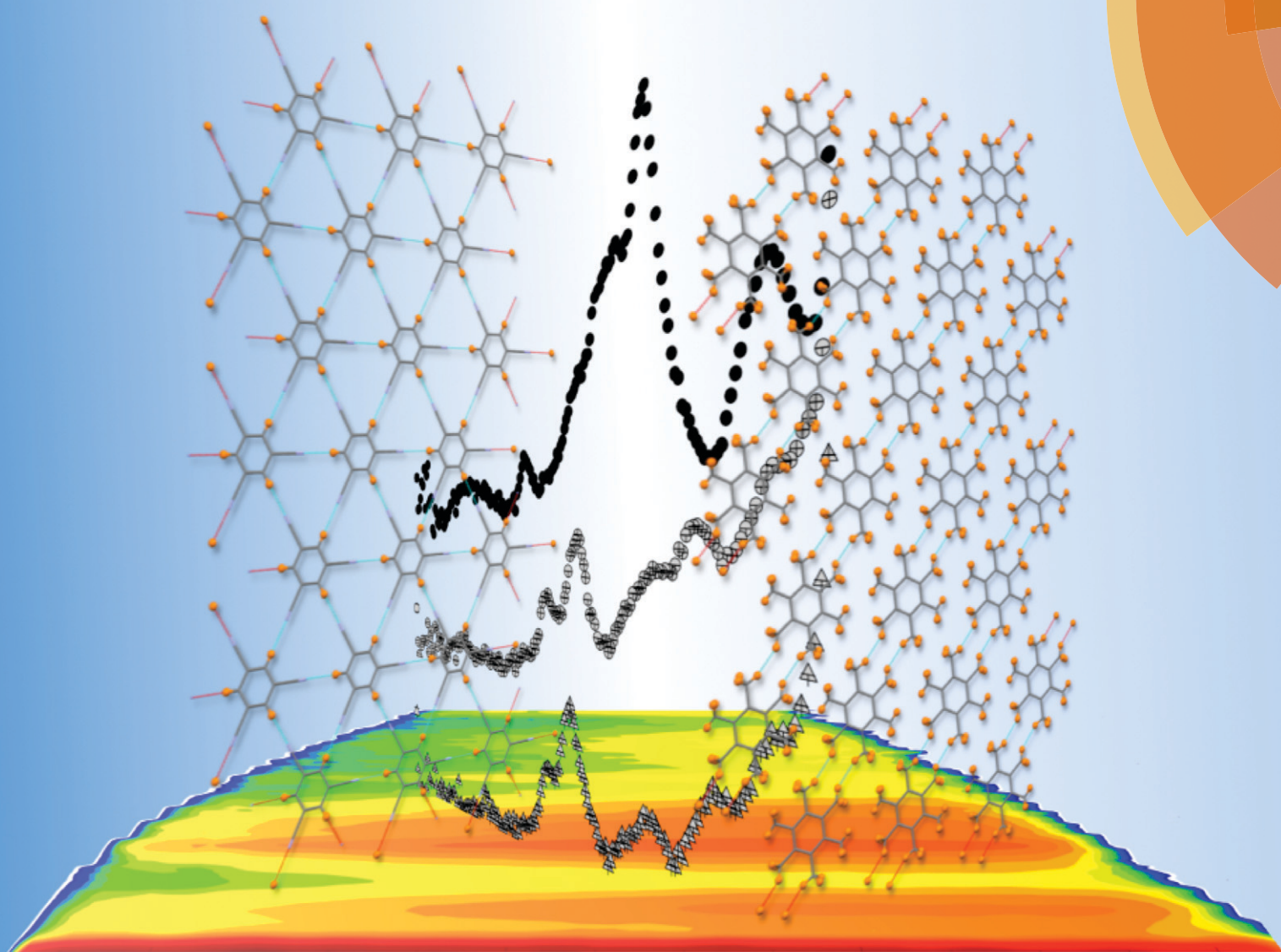


CrystEngComm

www.rsc.org/crystengcomm



PAPER

John A. Stride

Understanding the packing in the 1:1 molecular complex

1,3,5-tricyanobenzene–hexamethylbenzene by probing lattice modes

Cite this: *CrystEngComm*, 2015, 17, 3787Received 12th February 2015,
Accepted 11th March 2015

DOI: 10.1039/c5ce00328h

www.rsc.org/crystengcomm

Understanding the packing in the 1:1 molecular complex 1,3,5-tricyanobenzene–hexamethylbenzene by probing lattice modes†

John A. Stride^{ab}

The nature of hydrogen bonding and methyl group dynamics in the 1:1 molecular complex of hexamethylbenzene (HMB) and 1,3,5-tricyanobenzene (TCB) was probed using incoherent inelastic neutron scattering. The use of deuterated HMB allowed for the direct comparison of the methyl dynamics in the pure and complexed HMB molecules as well as directly observing changes to the hydrogen bonding about the TCB molecules.

1. Introduction

The physical and structural properties of the polymethylbenzenes have long been of interest to chemists as despite being small and relatively innocuous molecules of high ubiquity, they display a complexity in their intermolecular interactions that leads to solid–solid phase transitions in the pure materials and a range of molecular complexes, including π – π mediated charge transfer systems. Hexamethylbenzene (HMB) was one of the very first molecular materials to yield to single crystal structural determination,¹ closely following on from the first such determination, that of the highly symmetric structure of hexamethylenetetramine,² providing unambiguous evidence of the planarity of aromatic benzene rings for the first time. The structure of pentamethylbenzene (PMB) was reported for the first time only very recently;³ and both HMB and PMB have rich phase behaviours.^{3,4} However, in addition to the pure compounds, many aromatic systems display strong π – π interactions that can lead to charge transfer and electron hopping between donor and acceptor stacked species;⁵ such materials have undergone renewed interest of late due to their activity in the visible spectrum and room temperature ferroelectric behaviour.^{6,7} The polymethylbenzenes are the simplest members of this family of functionalized aromatics and many examples of donor–acceptor charge transfer species have been investigated in solution, with almost as many solid-state structures of binary systems

reported. One such notable material is the 1:1 complex of hexamethylbenzene and tricyanobenzene (HMB:TCB).⁸ Perhaps the most striking aspect of this material was that for the first time it demonstrated an interplay between the relatively weak C–H \cdots N hydrogen bond and the tendency to undergo π – π stacking, Fig. 1. The reported structure consists of interleaved planes of HMB and TCB occupying hexagonal arrays, arranged so as to maximize the π – π overlap between molecules in each layer. This is of note as whilst the structure of TCB is strongly hydrogen-bonded (mean $d_{\text{N-H}} = 2.506(54)$ Å), it is not arranged in planes of molecules, but rather, in off-set stacks that lie at 21° to each other, with hydrogen bonds out of the molecular planes and having the rather long π – π distance of 3.875 Å.⁹ Whilst the room temperature phase of HMB has planes of molecules, they are not arranged in columns of strong π – π interactions.¹⁰ However in HMB:TCB, all molecules lie almost perfectly in the planes parallel with (110), with a shorter π – π stacking distance of 3.615 Å and a mean hydrogen bond distance of $d_{\text{N-H}} = 2.542(1)$ Å.⁸ The driving force for the novel packing motifs of both HMB and TCB in the complex therefore appears to be the result of cooperative effects between the C–H \cdots N and π – π interactions. As a result, the intermolecular potentials, dominated here by the methyl group dynamics and the C–H \cdots N hydrogen bonds of the respective moieties, would be expected to differ markedly from that of the parent materials. Previous work by the author has reported the incoherent inelastic neutron scattering (IINS) spectrum of HMB in the phonon region, <50 meV (400 cm^{−1}),^{11,12} which is dominated by the methyl torsional modes; the question then is obvious – does incorporation of HMB into the HMB:TCB complexed solid perturb the methyl dynamics and if so how? In addition, what is the result of imposing planarity on the hydrogen-bonding dynamics of TCB?

^a School of Chemistry, University of New South Wales, Sydney, New South Wales 2052, Australia. E-mail: j.stride@unsw.edu.au

^b Bragg Institute, Australian Nuclear Science and Technology Organisation, Locked Bag 2001, Kirrawee DC, NSW 2232, Australia

† Electronic supplementary information (ESI) available. See DOI: 10.1039/c5ce00328h

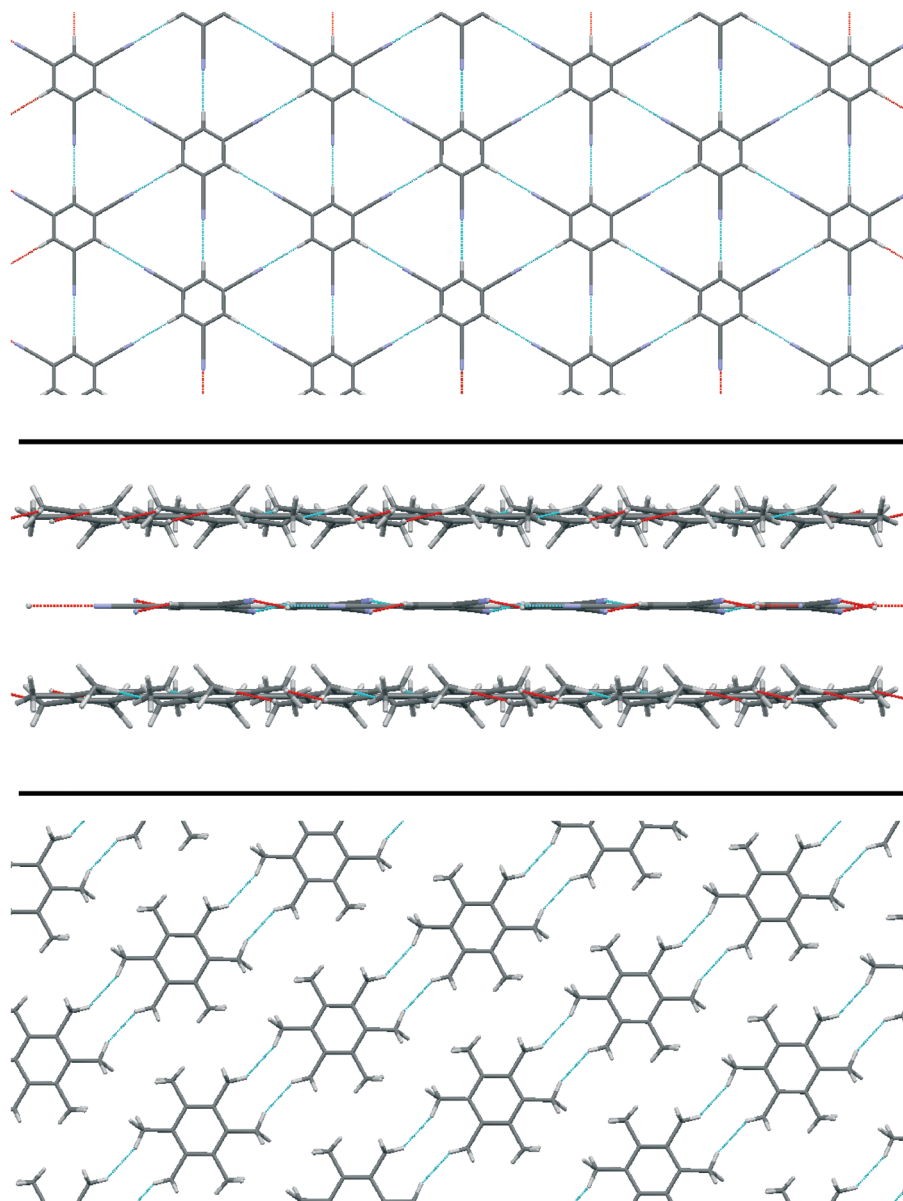


Fig. 1 Layered structure of HMB:TCB. Top: the C–H...N hydrogen bonded array of the TCB layers. Middle: view perpendicular to the layers showing strong interactions within the layers but relatively weak interactions between them; note that the structural fragment shown is of only three layers HMB:TCB:HMB. Bottom: the HMB array.

2. Experimental

INS measurements were performed on the IN4 thermal time-of-flight spectrometer at the ILL, France.¹³ Polycrystalline samples (0.39 g of $C_6(CH_3)_6:C_6H_3(CN)_3$; 1.9 g of $C_6(CD_3)_6:C_6H_3(CN)_3$ and 1.0 g $C_6H_3(CN)_3$; all of 99% purity) were placed into circular flat plate geometry Al cans of a sample thickness consistent with ~90% transmission (0.2 mm for HMB:TCB; 0.5 mm for TCB and 1 mm for d-HMB:TCB) and inserted into a cryostat to obtain the low sample temperatures at 135° to the incident beam, of wavelength $\lambda = 1.30$ Å, $E_i = 48.6$ meV. The data were collected over scattered angles of $18^\circ \leq 2\theta \leq 120^\circ$ at $T = 1.5$ K and manipulated using the LAMP routine.¹⁴

The 1:1 complexes were prepared by crystallisation from slowly evaporated equimolar solutions of the respective HMB and TCB prepared in a minimal quantity of $CHCl_3$ to yield dark blue crystals.

3. Results and discussion

IINS

The low energy phonon spectra of molecular species in incoherent inelastic neutron scattering are dominated by those modes involving appreciable hydrogen atom displacements in the course of the excitation. For example the spectrum of HMB is dominated by the methyl torsional modes that clearly have large associated hydrogen atom dynamics. For the



particular case of incoherent neutron scattering in the one-phonon approximation, the intensity, I , can be represented as:¹⁵

$$I \propto S_{\text{inc}}(Q, \omega) \propto \sigma Q^2 \exp\left(-\frac{Q^2 \langle u^2 \rangle}{3}\right) \frac{n(\omega) + 1}{\omega} g(\omega)$$

where σ is the total neutron scattering cross-section of the molecule, $n(\omega)$ is the Bose occupation factor and $\langle u(T)^2 \rangle$ is the mean square displacement of the atoms and $g(\omega)$ is the density of states. The incoherent cross-section of protons is $80.26 \times 10^{-24} \text{ cm}^2$, around an order of magnitude larger than any other cross-section in the samples studied; as such the measured spectra are heavily proton-weighted and so to a first approximation, only proton motions need be considered in $g(\omega)$. Another facet of IINS that was utilised in this work is the isotopic variance of the scattered intensities courtesy of the difference in the incoherent neutron scattering cross-sections of isotopes of the same element; for example deuterium has an incoherent cross-section of $2.05 \times 10^{-24} \text{ cm}^2$, only 2.6% that of hydrogen. In this case, by deuterating at the hydrogen positions of HMB, the cross-section associated with those modes was effectively silenced. The shift brought about by the increased mass is insignificant when compared with the dramatic decrease in spectral intensity. By measuring spectra of HMB:TCB, d-HMB:TCB and TCB under identical conditions, then the hydrogen modes of TCB in d-HMB:TCB were directly observed, whilst the difference spectrum of [HMB:TCB – d-HMB:TCB] should yield only the hydrogen spectrum of the HMB molecules in the complex.

TCB

The phonon spectrum up to 40 meV (320 cm^{-1}) of TCB is dominated by two features at 22.2 and 24.6 meV (179 and 198 cm^{-1} , respectively), Fig. 2. The intensity of these modes increased as a function of Q , Fig. S1, ESI†, consistent with them being wholly vibrational or phonon modes. Displayed as a density of states summed across the Brillouin zone, Fig. 2, then at least three weaker features are also evident at 5.4, 9.6 and 14.8 meV. The lowest energy features are consistent with them being due to acoustic phonons, exemplified by their broad peak shapes. Whilst the peak at 14.8 meV is likely to be due to a molecular motion, the hydrogen-weighting of the peak makes it more likely to be a conformational twisting of the benzene ring with an associated relatively small hydrogen atom displacement. In contrast, the dominant peaks at 22.2 and 24.6 meV are clearly strongly hydrogen-centered and are assigned to an in-plane and out-of-plane deformation across the C–H⋯N hydrogen bond and as such should be sensitive to the H-bonding regime.

d-HMB:TCB

Again the phonon spectrum up to 40 meV (320 cm^{-1}) is dominated by two features, however these are both shifted relative to TCB, lying at 21.4 and 24.8 meV (173 and 200 cm^{-1} ,

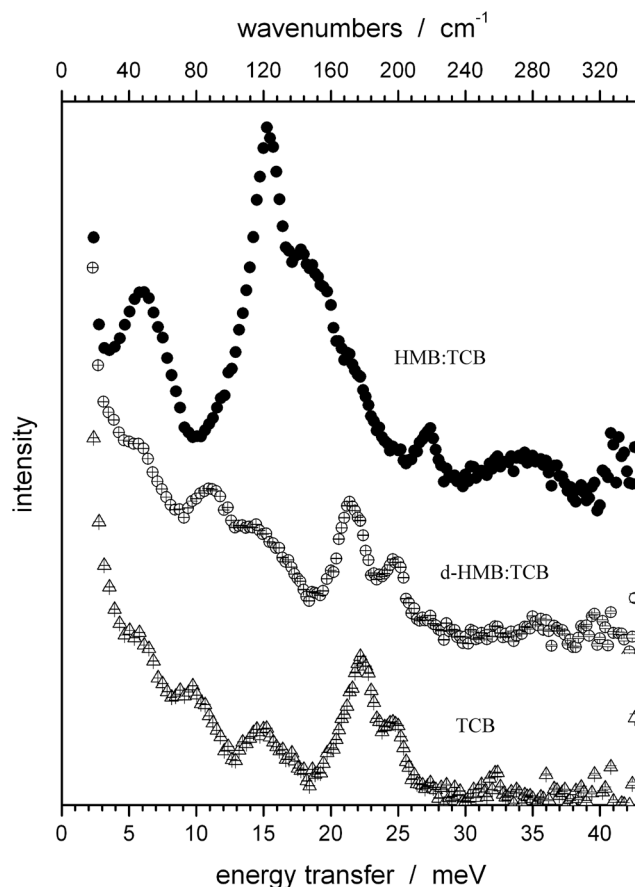


Fig. 2 Incoherent inelastic neutron scattering spectra of HMB:TCB (top), d-HMB:TCB (middle) and TCB (bottom) obtained on IN4 at $\lambda_i = 1.30 \text{ \AA}$ ($E_i = 48.6 \text{ meV}$) and 1.5 K . All spectra are displayed on a common intensity scale, vertically off-set for clarity.

respectively), Fig. 2. The increasing intensity of these modes as a function of Q , Fig. S1, ESI†, shows them to be wholly vibrational or phonon modes. The small energy shifts of -0.8 and $+0.2 \text{ meV}$ relative to pure TCB are a direct consequence of the different H-bonding environments in the two structures. In TCB the H-bonds are non-planar with respect to the aromatic rings, having a mean bond angle across the C–H⋯N units of $156(8)^\circ$; as such displacements of hydrogen will lie in a more isotropic potential, limiting any splitting in the so-called in-plane and out-of-plane modes. In contrast, the HMB:TCB complex has planes of H-bonded TCB molecules with the mean C–H⋯N bond angles of $174(5)^\circ$, for which a clear demarcation between in-plane and out-of-plane modes can be made; accordingly, the hydrogen atom displacements will be significantly more anisotropic, in this case around 96.5 Jmol^{-1} . The spectral evidence supports this, with the more intense in-plane mode shifting down in energy and the out-of-plane mode undergoing a small blue-shift. Given that the mean H-bond distance increases in going from TCB to HMB:TCB, from $d_{\text{N-H}} = 2.506(54) \text{ \AA}$ to $d_{\text{N-H}} = 2.542(1) \text{ \AA}$, an associated weakening of the interaction acts to limit the extent of the red and blue shifts observed for the more planar H-bonding network in the 1:1 complex.



The acoustic phonon modes of d-HMB:TCB are present at 5.1 and 11.0 meV, although here they relate to the lattice of the complex, which having more molecules per unit cell, equates to broader features. The mode at 14.4 meV appears to be consistent with that observed at 14.8 meV in TCB and is assigned to a molecular deformation; in which case a shift of -0.4 meV reflects a relaxed intermolecular potential of 39 Jmol^{-1} in the complex relative to pure TCB.

HMB:TCB

With the large increase in hydrogen-content over both TCB and d-HMB-TCB, the HMB-TCB spectrum up to 40 meV (320 cm^{-1}) is dominated by the methyl torsions at 15.3 and 17.8 meV, which as to be expected yield significantly more inelastic intensity than either of the other two samples, Fig. 1 with the Q -dependence shown in Fig. S1.† Despite this, the familiar features of the TCB spectrum at 20–25 meV can also be seen as a high energy shoulder to the methyl torsions. By taking the difference between the HMB:TCB and d-HMB-TCB, the contributions from the TCB can be eliminated, to arrive at only the spectrum of the HMB molecules within the HMB:TCB complex, Fig. 3. This is of interest as a comparison to data obtained under the same conditions for pure HMB then highlights just how the methyl torsions are affected by inclusion into the binary complex. The methyl torsions of HMB split into two broad branches under the experimental resolution, which have been shown by *ab-initio* calculations to be due to populations of discrete geared torsional modes, with the lowest lying mode being that of the fully-gear

rotations.¹² Experimentally these modes were manifest as two features at 15.6, 19.6 meV, both higher in energy than in the complexed species. In itself this is notable inasmuch as the IINS spectrum of HMB can be envisaged, to a first approximation, as being intramolecular in nature – the gearing of six methyl groups located on a single aromatic ring. However, this finding clearly demonstrates that there is appreciable intermolecular influence on these modes, consistent with the requirement of undergoing a relatively large structural displacement such as a torsional motion. Perhaps not surprisingly the fully-gear motions are less influenced by intermolecular forces due to the weaker external perturbation that such motions exert relative to the out of phase motions (shift of -0.3 meV vs. 1.8 meV). It is notable that all of the methyl modes in the complexed HMB are relaxed relative to those in pure HMB.

The observed acoustic phonon modes in HMB:TCB are essentially those relating to the HMB sites simply as a result of the greater spectral weight associated with the number of hydrogen atoms present, Fig. 2. Indeed, even in the difference spectrum, Fig. 3, there is little to differentiate the acoustic phonons in the vibrational density of states of HMB:TCB to those in pure HMB at this resolution (Fig. 4).

Hirshfeld surfaces

Analysis of the Hirshfeld surfaces of molecules in both TCB and the HMB:TCB complex using the CrystalExplorer software^{16,17} highlights the dominant interactions and provides additional insight into the IINS data. In pure TCB, each molecule sits in a highly symmetric site, strongly hydrogen bonded to three neighbouring molecules through a donor $\text{C-H}\cdots\text{N}$ interaction and three molecules in an acceptor $\text{N}\cdots\text{H-C}$ interaction. The main intermolecular interactions are those hydrogen bonds, consisting of 50% of the total Hirshfeld surface, with both $\text{C}\cdots\text{C}$ and $\text{N}\cdots\text{N}$ interactions each making up 13%. The remaining surface comprises small contributions from $\text{C}\cdots\text{N}$, $\text{C}\cdots\text{H}$ and $\text{H}\cdots\text{H}$ interactions, the latter being only $<1\%$. However, when TCB is incorporated into the HMB:TCB structure, then the Hirshfeld surface is radically different, with hydrogen bonding interactions accounting for 55% of the surface. The $\text{C}\cdots\text{H}$ contacts make up 18% of the surface and hydrogen-hydrogen contacts increase to 16%. This shift in the weighting of the intermolecular interactions is evident in the fingerprint plots, with far more pronounced fingers that relate to the hydrogen bond extending to lower *de* and *di*. The fact that hydrogen interactions outside of the hydrogen bonds consist of only 9.3% and 34.1% of the surfaces of the pure and complexed TCB molecules is consistent with the hydrogen bond being dominant in the IINS response.

The Hirshfeld surface of HMB has been shown previously to consist of 82% $\text{H}\cdots\text{H}$ and 18% $\text{C}\cdots\text{H}$ contributions;² however in the complexed molecule, additional interactions are present and the $\text{H}\cdots\text{H}$ contribution falls to 58%, with other major constituents being the $\text{H}\cdots\text{N}$ and $\text{H}\cdots\text{C}$ interactions of

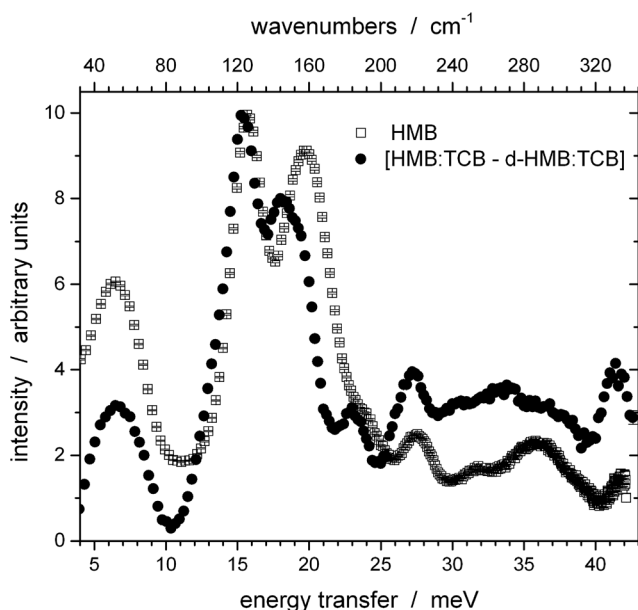


Fig. 3 Difference spectrum of HMB in HMB:TCB (closed circles) compared to the incoherent inelastic neutron scattering spectra of pure HMB (open squares). All data obtained on IN4 at $\lambda_i = 1.30 \text{ \AA}$ ($E_i = 48.6$ meV) and 1.5 K. Difference spectrum refers to the subtraction of the spectrum of d-HMB:TCB from HMB:TCB.



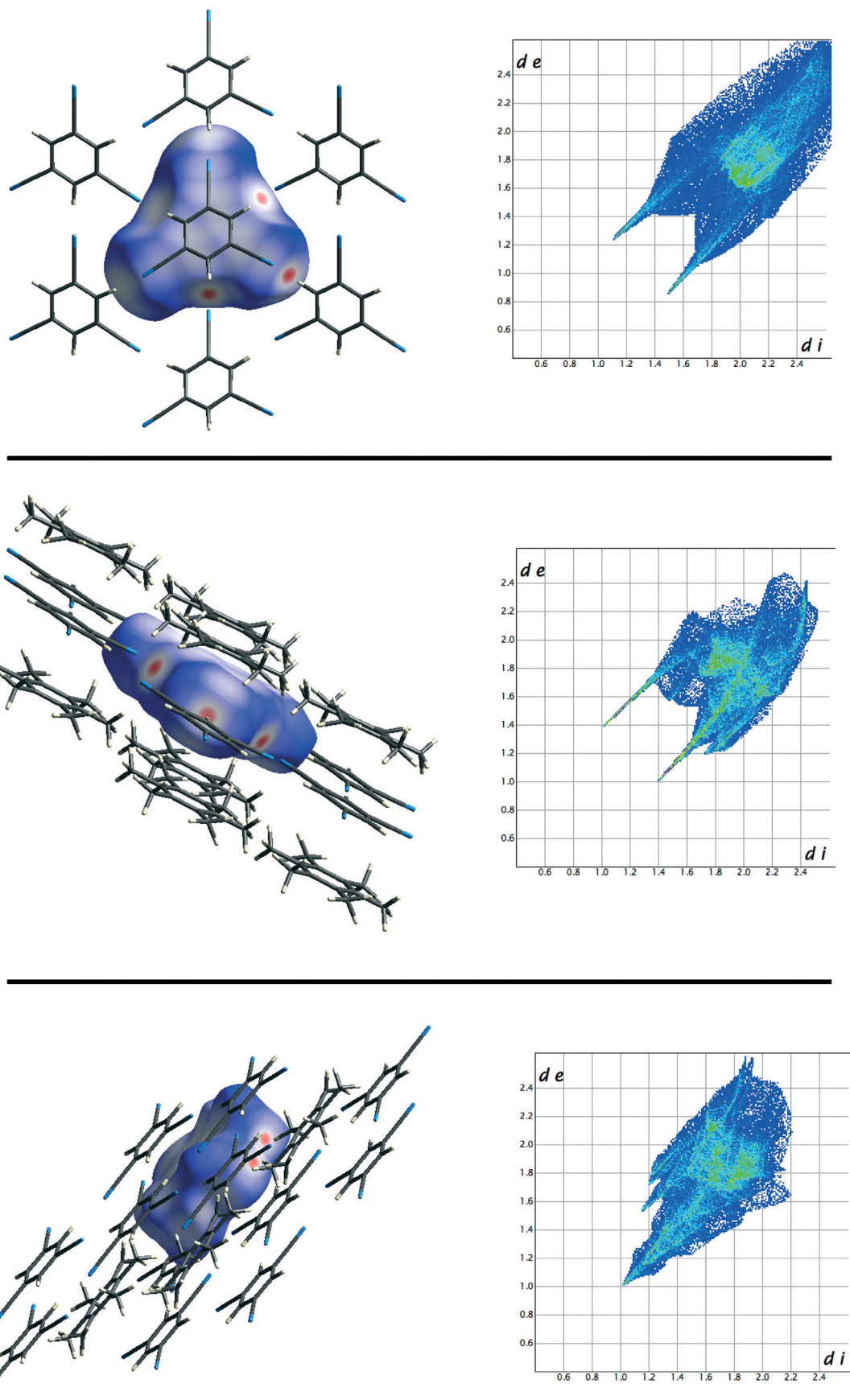


Fig. 4 Hirshfeld surfaces (left hand-side) and fingerprint plots (right hand-side) of HMB and TCB. Top: TCB. Middle: TCB in HMB:TCB. Bottom: HMB in HMB:TCB. All surfaces are shown on a common scale of: -0.262 Å (red) to $+1.395$ Å (blue) relative to the Hirshfeld surface.

19% and 13% respectively. This decrease in the H...H interaction represents a relaxation of the intermolecular contribution to the methyl dynamics as of course in HMB, all hydrogen molecules relate to methyl groups. This then augments the observation that the methyl groups in the complexed HMB molecules have lower energy torsional modes.

4. Conclusion

The use of a deuterated sample of HMB in the study of the intermolecular complex HMB:TCB allowed for the elucidation of the effects of complexation on both the HMB and TCB molecules. Whilst the hydrogen bonds of TCB in HMB:TCB are longer than in the pure material, they are more coplanar with the molecules, resulting in marked shifts of the hydrogen bond deformation observed in the IINS spectra. Whilst the effects of this are significant, the absolute magnitude associated with the hydrogen bond deformation is not dramatically perturbed. Perhaps more of an effect was observed in the methyl torsions of HMB. By comparing the difference spectrum obtained by subtracting the d-HMB:TCB spectrum from the HMB:TCB spectrum, with that of pure HMB, a pronounced intermolecular contribution to the methyl torsions was observed. In essence the less-densely packed HMB molecules in the complex more readily undergo methyl torsions, with the effect more pronounced in the less coherent gearings about the ring, which incur greater local perturbations of the molecular environment of HMB.

Acknowledgements

The author would like to thank staff of the Institut Laue-Langevin, Grenoble, France for access to neutron beam time. I would like to thank one of the referees for bringing ref. 2 to my attention and adding to my knowledge of the early days of crystallography.

References

- 1 K. Lonsdale, *Trans. Faraday Soc.*, 1929, 25, 352–366.
- 2 R. Dickinson and A. L. Raymond, *J. Am. Chem. Soc.*, 1923, 45, 22–29.
- 3 J. A. Stride, *Acta Crystallogr., Sect. B: Struct. Sci.*, 2005, 61, 200–206.
- 4 M. Mudge, B. K. Ng, C. J. Onie, M. Bhadbhade, R. A. Mole, K. C. Rule, A. P. J. Stampfl and J. A. Stride, *ChemPhysChem*, 2014, 15, 3776–3781.
- 5 A. A. J. Aquino, I. Borges Jr., R. Nieman, A. Köhn and H. Lischka, *Phys. Chem. Chem. Phys.*, 2014, 16, 20586–20597.
- 6 U. M. Rabie, *J. Mol. Struct.*, 2013, 1034, 393–403.
- 7 A. S. Tayi, A. K. Shveyd, A. C.-H. Sue, J. M. Szarko, B. S. Rolczynski, D. Cao, T. J. Kennedy, A. A. Sarjeant, C. L. Stern, W. F. Paxton, W. Wu, S. K. Dey, A. C. Fahrenbach, J. R. Guest, H. Mohseni, L. X. Chen, K. L. Wang, J. F. Stoddart and S. I. Stupp, *Nature*, 2012, 488, 485–489.
- 8 D. S. Reddy, B. S. Goud, K. Panneerselvam and G. R. Desiraju, *J. Chem. Soc., Chem. Commun.*, 1993, 663–664.
- 9 D. S. Reddy, K. Panneerselvam, G. R. Desiraju, H. L. Carrell and C. J. Carrell, *Acta Crystallogr., Sect. C: Cryst. Struct. Commun.*, 1995, 51, 2352–2354.
- 10 P. Le Maguères, S. V. Lindeman and J. K. Kochi, *Organometallics*, 2001, 20, 115–125.
- 11 J. M. Adams, A. S. Ivanov, M. R. Johnson and J. A. Stride, *Phys. B*, 2004, 350, E351–354.
- 12 J. A. Stride, J. M. Adams and M. R. Johnson, *Chem. Phys.*, 2005, 317, 143–152.
- 13 G. Cicognani, H. Mutka and F. Sacchetti, *Phys. B*, 2000, 276–278, 83–84.
- 14 LAMP, the Large Array Manipulation Program, http://wwwold.ill.fr/data_treat/lamp/lamp.html.
- 15 S. W. Lovesey, in *Theory of Neutron Scattering from Condensed Matter*, Clarendon, Oxford, 1984.
- 16 M. A. Spackman and D. Jayatilaka, *CrystEngComm*, 2009, 11, 19–32.
- 17 J. J. McKinnon, D. Jayatilaka and M. A. Spackman, *Chem. Commun.*, 2007, 3814–3816.

